Fluorinated-Plasma Modification Of Polyetherimide Films

Meriyam Kaba,[1,2] Azzouz Essamri,[1] Andre Mas,[2] Francois Schue,[2] G. A. George,[3] F. Cardona,[3] L. Rintoul,[4] B. J. Wood[5]

[1]*Laboratoire de Génie des Procédés, Faculté des Sciences, Université Ibn Tofail, BP 133, 14000 Kenitra, Morocco*
[2]*Organisation Moléculaire Evolution et Matériaux Fluorés, UMR CNRS 5073, Université Montpellier II, 34095 Montpellier Cedex 05, France*
[3]*School of Physical Sciences, Queensland University of Technology, Garden Points, Queensland 4001, Australia*
[4]*Centre for Instrumental and Developmental Chemistry, Queensland University of Technology, Brisbane, Queensland 4001, Australia*
[5]*Department of Chemistry, The University of Queensland, Brisbane, Queensland 4072, Australia*

Received 8 December 2004; accepted 22 April 2005
DOI 10.1002/app.22930
Published online in Wiley InterScience (www.interscience.wiley.com).

ABSTRACT: Ultem 1000 polyetherimide films prepared by cast-evaporating technique were covered with a 1*H*,1*H*,2*H*-tridecafluoro-oct-1-ene (PFO) plasma-polymerized layer. The effects of the plasma exposure time on the surface composition were studied by X-ray photoelectron spectroscopy, Fourier transform infrared spectroscopy, and surface energy analysis. The surface topography of the plasma layer was deduced from scanning electron microscopy. The F/C ratio for plasma-polymerized PFO under the input RF power of 50 W can be as high as 1.30 for 480 s and ~0.4–2 at % of oxygen was detected, resulting from the reaction of long-lived radicals in the plasma polymer with atmospheric oxygen. The plasma deposition of fluorocarbon coating from plasma PFO reduces the surface energy from 46 to 18.3 mJ m^{-2}. © 2006 Wiley Periodicals, Inc. J Appl Polym Sci 100: 3579–3588, 2006

Key words: plasma polymerization; fluoropolymer; X-ray photoelectron spectroscopy; polyimide

INTRODUCTION

Any problems of pollution of our planet encourages us to find new techniques that have, as a priority, the respect of the cleanliness of our environment, in substituting the classic methods of chemical modification of polymeric surface by nonpolluting techniques. Processes of surface treatment by cold plasma are among the best techniques.

The surface treatment by plasma allows us to obtain a large variety of chemical structures. These changes of surface properties can be achieved by simple variation of the experimental parameters of treatment, the nature and the proportion of gases and monomers used.

Plasma polymerization (PP) is a solvent-free, room temperature process that can be used to rapidly deposit thin polymer films onto a wide variety of substrates.[1,2] In PP, a neutral "monomer" gas or vapor in a low pressure reactor is subjected to an electric field. The monomer is fragmented into reactive species, which subsequently recombine, forming a crosslinked polymer. The monomers can be hydrocarbon, fluorocarbon, organosilicon, or organometallic, and do not necessarily need to include the functional groups typically associated with conventional polymerization techniques.[1] The molecular structure and properties of the plasma polymer depend on the monomer nature and flow rate, plasma power, and reactor pressure. The advantages of PP include the environmental friendliness of the solvent-free process, the deposition of ultra-thin films with thickness directly proportional to deposition time, the deposition of highly adherent films with substrate activation in the plasma environment, the plethora of monomers available, and the simplicity of the reactor.

This technique is widely used in polymer adhesion, biomaterial compatibility, and membrane separation domain. To improve the transport properties of a gas and liquid separation membrane, particularly to enhance the hydrophobicity, the surface can be modified by exposure to fluorinated compound monomers. A thin coating of fluorinated polymer is formed on the surface of the homogeneous separation layer or skin of the membrane. The chemical composition and depth of the fluorinated layer depend essentially on the treatment conditions, in particular the fluorine concentration in the reactor and the fluorination time.

A number of excellent studies dealing with the PP of fluorine-containing monomers to produce fluoropolymer films with ultra-hydrophobic properties have appeared recently.[3,4] Fluoromonomers, including perfluoroallylbenzene,[3] pentafluorostyrene,[5] 1*H*,1*H*,2*H*-perfluoro-1-decene,[6] 1*H*,1*H*,2*H*,2*H*-heptadecafluorodecyl

Correspondence to: F. Schue (schue@univ-montp2.fr).

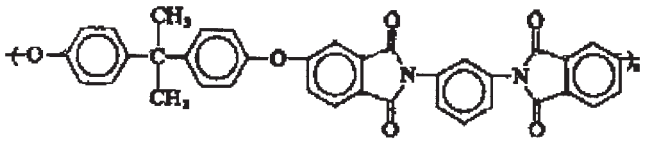

Scheme 1 Ultem 1000 (PEI).

acrylate,[7] and 2,2,3,3,4,4,4-heptafluorobutyl acrylate[8] have been employed.

The objective of this work is the treatment of the surface of Ultem 1000 (PEI) films by fluorinated plasma using 1*H*,1*H*,2*H*-tridecafluoro-oct-1-ene monomer (the formula is CF_3—$(CF_2)_5$—CH═CH_2 and it is called perfluorooctene (PFO) in the present article) to increase their hydrophobicity, and to develop their application in pervaporation for the separation of the organic mixtures and for the extraction of volatile organic micropolluants from water.

In the present work, PFO was plasma-polymerized (pp-PFO coating) and deposited on an Ar plasma-pretreated PEI surface, leading to pp-PFO-PEI surface. The PFO molecule contains a reactive vinyl group and a stable fluorinated group. A highly fluorinated and hydrophobic film can thus be deposited. The effects of the glow discharge parameters on the surface composition and the topography of the pp-PFO-PEI surfaces were characterized by X-ray photoelectron spectroscopy (XPS), Fourier transform infrared in the attenuated total reflectance mode (FTIR-ATR) spectroscopy, scanning electron microscopy (SEM), and surface energy analysis.

EXPERIMENTAL

Materials and methods

The polyetherimide (PEI) used in this study is a product of General Electric Plastics, The Netherlands, and is marketed under the trade name Ultem 1000. The glass transition temperature is 217°C and the chemical structure is given here (Scheme 1). *N*-Methyl-2-pyrrolidinone (NMP) (Sigma-Aldrich, France) was used as solvent for the preparation of the membrane casting solution.

The monomer used for plasma polymerization (PP) is 1*H*,1*H*,2*H*-tridecafluoro-oct-1-ene (PFO, Lancaster, 97%).

Membrane preparation

The polyetherimide material was dissolved in NMP at 90°C for 4 h to obtain a 6 wt % homogeneous solution. The polymer solution was cast at room temperature on a glass plate. The cast film was then quickly placed into a vacuum oven for 4 h at 70°C to evaporate the NMP solvent. The membranes and films were solvent casted to avoid any trace of potential contaminants and used to study the effects of the plasma treatment on the polymer surface.[9]

Plasma polymerization of PFO: the pp-PFO coating

A glass bell-jar reactor containing two parallel plate electrodes (3 cm apart) and powered by an RF generator (13.56 MHz) was used. PFO was used as a liquid and evaporated into the reactor at a rate controlled by the operating pressure. A scheme of the plasma treatment experimental set-up is shown in Figure 1. Prior to the plasma treatment, the substrates were dried under vacuum and then submitted to an argon plasma pretreatment (50 W, 40 Pa, 4.7 sccm) for 2 min to clean their surfaces. Then vacuum was established in the reaction chamber for 5 min to evacuate the volatilized degradation products, the PFO monomer vapor flow was regulated to obtain the desired pressure (40 Pa), and the PFO was allowed to flow in. Only then, the 50 W RF power was applied to generate the plasma glow discharge for various treatment times from 10–480 s.

X-ray photoelectron spectroscopy

The XPS spectra were obtained using a PerkinElmer, Physical Electronics Industries (PHI) Model 560 using Mg Kα exciting radiation (1253.6 eV). Typically, the X-ray gun was operated at 15 kV and 400 W. The system incorporates a PHI Model 25–270 AR electron energy analyzer with an average take-off angle (reference to the sample normal) of 37.7°. The sample chamber was evacuated to 10^{-7} Torr before the sample was

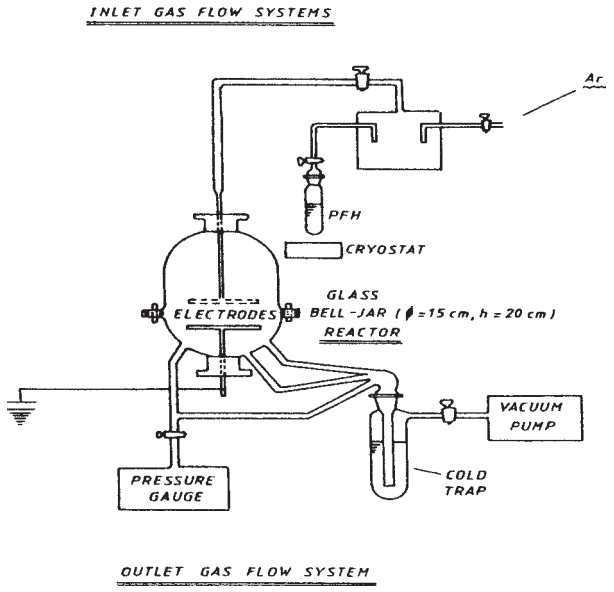

Figure 1 Scheme of the experimental set-up used for the plasma treatments.

introduced and an ion pump was used to maintain the low vacuum required for analysis. The pressure during spectral acquisition was between 5×10^{-7} and 5×10^{-8} Torr.

All binding energies (BEs) were referenced to the C—C/C—H carbon peak at 285.0 eV. With data processing involving curve fitting, the line width (full width at half maximum, or FWHM) for the Gaussian peaks was maintained constant at 1.7 eV for all components in a particular spectrum, and the Gauss–Lorentzian shape ratios of individual peaks were fixed at 90% Gaussian.

Fourier transform infrared spectroscopy

Infrared spectra were obtained by making contact between the sample and a slide-on silicon attenuated total reflectance (ATR) objective of a Continuum microscope attached to a Nicolet Nexus 870 bench (Nicolet Instrument Corp., Madison, WI). Spectra were collected using a nominal 100×100 μm^2 aperture in the spectral range 4000–700 cm^{-1} with 128 scans at 4 cm^{-1} resolution and a mirror velocity of ~2 cm s^{-1}. Mapping was performed using the auto-mapping function of the Nicolet Atlus software. In each measurement cycle, the stage is automatically raised until contact is made between the sample and the ATR objective as monitored by a contact alert device. The spectrum is then recorded before the stage is lowered and the sample moved by a 50 μm increment. By repeating this process in a raster fashion, a spectral map comprising 121 spectra was obtained for a total area of 500×500 μm^2. Although a nominal 100×100-μm^2-aperture was used, the effective area under analysis at each mapped point is approximately the nominal aperture divided by the refractive index (RI) of the internal reflection element (IRE). Si has an RI of 3.4, and so in this case the effective aperture size is $\sim 30 \times 30$ μm^2. A background was recorded prior to every third spectrum.

Spectral data manipulations were performed using either the Nicolet OMNIC 5.2a program or GRAMS 32 software package (version 4.01, level 1, 1996, Galactic Industries Corp, Salem, NH). Chemometric calculations were performed using the Nicolet TQ Analyst software package.

Contact angle measurements

Static measurements of the contact angle were made with a Kruss G1 apparatus. The polymer films were placed on a metallic support and the measurements were made with water and diiodomethane at 25°C. The method developed by Owens and Wendt[10] allowed to calculate the surface energy γ_S of polymers using the relations:

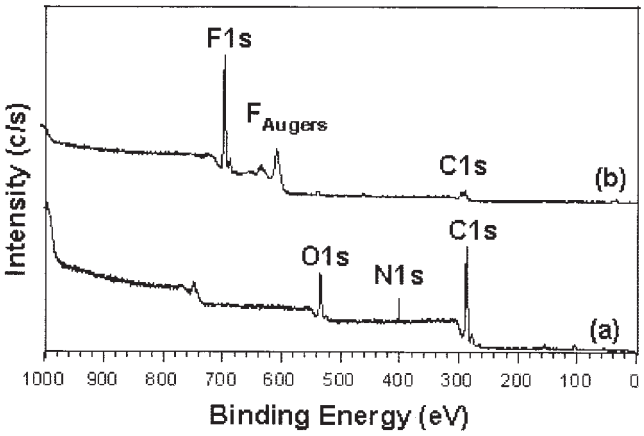

Figure 2 XPS broad scan spectra of PEI before (a) and after pp-PFO treatment for 10 s (b).

$$(1 + \cos\theta)\gamma_L = 2(\gamma_S^d \gamma_L^d)^{1/2} - 2(\gamma_S^p \gamma_L^p)^{1/2}$$

and

$$\gamma_S = \gamma_S^p + \gamma_S^d$$

where γ_S^d and γ_S^P are respectively the dispersive and polar components of the surface, θ is the contact angle, $\gamma_{L(H_2O)} = 78.8$ mJ m^{-2}, $\gamma_{L(CH_2I_2)} = 50.8$ mJ m^{-2} the superficial tensions of the liquids, $\gamma^d_{L(H_2O)} = 21.8$ mJ m^{-2}, $\gamma^d_{L(CH_2I_2)} = 49.5$ mJ m^{-2} their dispersive components, and $\gamma^p_{L(H_2O)} = 51$ mJ m^{-2}, $\gamma^p_{L(CH_2I_2)} = 1.3$ mJ m^{-2} their polar components.

Scanning electron microscopy

Scanning electron micrographs photographs were obtained using a Jeol JSM 35 apparatus. Treated films were broken in liquid nitrogen for a better analysis of the cross section and to enable the estimation of the thickness of the fluorocarbon coating.

RESULTS AND DISCUSSION

Fluorination of PEI

As discussed earlier, fluorination of the exposed membrane surface creates a fluorinated layer on the Ultem 1000. Other effects may include crosslinking and disruption of the polymer backbone. The fluorination conditions determine the thickness, chemical nature, and uniformity of this layer, and XPS was used to probe the surface composition.

Figure 2 shows a broad scan spectrum of PEI before (a) and after mild fluorination for 10 s with PFO plasma treatment (b). In both spectra the peaks for carbon (C1s), nitrogen (N1s), and oxygen (O1s) were identified at their characteristic BEs of about 285, 400, and 533 eV, respectively. The spectrum shows the appearance of the F1s

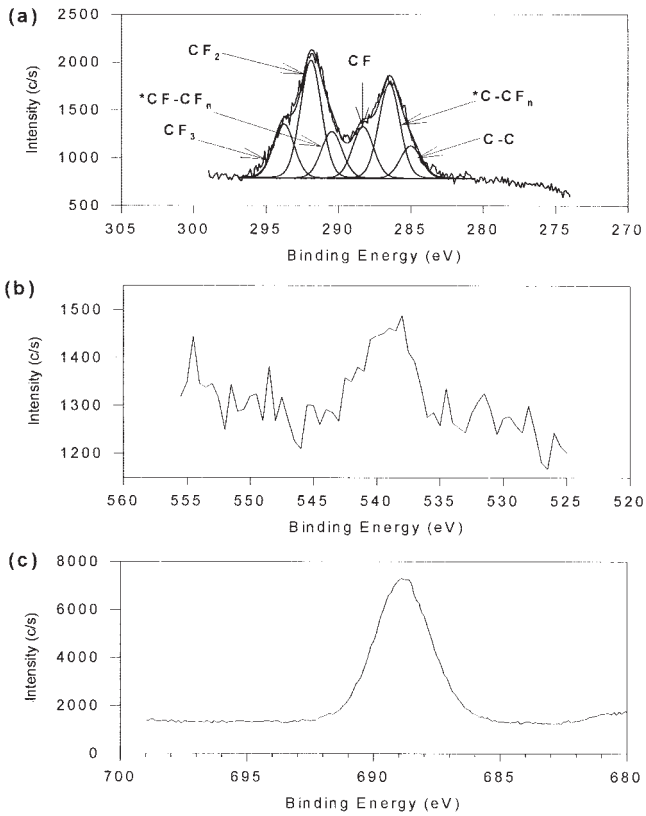

Figure 3 The XPS spectra for C1s (a), O1s (b), and F1s after pp-PFO for 10 s (c).

(695 eV) and F Auger (597 eV) peaks after fluorination,[11,12] indicating the presence of a fluoropolymer on the surface of the PEI. The disappearance of N1s component gives information about the thickness of the fluorinated deposit, which is higher or equal to the analyzed depth estimated at 10 nm.

High-resolution XPS spectra corresponding to a pp-PFO-PEI (10 s, 50 W, 40 Pa) with an electron take-off angle of 37.7° is shown in Figure 3. The interpretation of the signal F1s and O1s scans is straightforward. The F1s [Fig. 3(c)] consists of a single symmetrical peak, which proves that XPS does not make it possible to highlight its chemical environment. The O1s peak [Fig. 3(b)] with a low intensity corresponds to the different types of oxygen atoms in the pp-PFO and can be assigned to the reaction of plasma polymer radicals with atmospheric oxygen.[13,14]

The nature of the changes on the surface is also reflected by the changes in the C1s spectra. The deconvoluted C1s spectra were used to quantitatively investigate the chemical structure of the plasma-fluorinated films from PFO.

The C1s peak shown in the Figure 3(a) reveals complex signals extending over an energy interval of ~12 eV. We found six chemically differently bonded carbon atoms present in the pp-PFO-PEI, according to the curve-fitting procedures.

These peaks are quite broad, with an average full width at half-maximum (FWHM) of 1.7 eV. This can likely be attributed to the multiple electronic environments created by the addition of fluorine to carbon atoms.

The curve fits for plasma fluoro polymer C1s spectra in literature usually include CF_3, CF_2, CF, and *C—CF peaks and, in some cases, a C—C peak.[1,15] There is no regular molecular structure in this random addition of monomer fragments, and therefore, the molecular environments of identical groups may be quite varied.

The binding energy peak positions were determined for the plasma polymerized fluorocarbons using the C1s spectra of the pp-PFO-PEI (50 W, 10 s, 40 Pa) in Figure 3(a). Using the peak at 285 eV as a reference, BEs were assigned to other pp-PFO peak. The peak at the highest binding energy, 293.80 eV, was assigned to CF_3. The peak with the second highest binding energy, 291.70 eV, (and the highest magnitude) was assigned to CF_2. These peak positions and the 2.1 eV difference between them are similar to those found in the literature.[16]

The binding energy peak positions were determined for the plasma-polymerized fluorocarbons. The peaks at 290.46, 288.30, and 286.48 eV were assigned to *CF—CF_n, CF, and *C-CF_n, respectively, in accordance with other plasma fluoro polymer XPS studies in the literature.[17]

*CF—CF_n and *C—CF_n represent, respectively, monofluorinated carbon and nonfluorinated carbon affected by a neighborhood of highly fluorinated carbon.

Surface composition of the plasma-polymerized PFO on the plasma-pretreated PEI films (pp-PFO-PEI films)

XPS reveals significant changes on the surface with increasing exposure time to PFO plasma (50 W, 40 Pa). The variations in elemental composition, as determined from the XPS spectra, are given in Table I (where percentage is the atomic concentration of each

TABLE I
XPS Elemental Analysis of PEI Following Various PFO Plasma Exposure Times

Exposure time (s)	Chemical composition (%)				
	C	F	O	N	F/C
0	83.0	—	14.0	3.0	0
10	46.5	52.3	1.2	—	1.12
30	47.5	51.3	1.2	—	1.08
60	43.7	54.3	2.0	—	1.24
120	44.4	55.2	0.4	—	1.24
240	43.4	55.8	0.8	—	1.28
480	43.0	55.9	1.1	—	1.30

Plasma treatment: 50W, 40Pa.

TABLE II
Peak Contributions to CIs Spectra for Various PFO Plasma Exposure Times

Exposure time (s)	% of atomic groups					
	C—C	C*—CF_n	CF	*CF—CF_n	CF_2	CF_3
10	8.2	23.9	13.0	11.7	29.6	13.6
30	8.6	22.7	12.8	10.0	30.3	15.6
60	13.7	21.8	10.4	17.2	24.9	12.0
120	9.6	21.6	11.6	13.5	29.6	14.1
240	9.0	22.0	11.3	11.5	32.0	14.2
480	7.5	21.9	12.1	15.6	30.4	12.5
% average value	9.5	22.3	11.9	13.2	31.1	13.7

element). The XPS characterization shows that the oxygen, carbon, and nitrogen contents decrease, and the fluorine content increases, with the increase in PFO plasma exposure time.

The low oxygen content is typical of plasma fluoropolymers: the incorporated oxygen coming from the reaction of plasma polymer radicals with atmospheric oxygen. The presence of oxygen after fluorination has been reported by several independent researchers.[18–20] Mohr et al.[20] specially investigated the origin of the oxygen in a series of controlled fluorination experiments and came to the conclusion that oxygen must be present as a contaminant in the dissolved liquid monomers. The contaminants were indicated to be mainly oxygen and nitrogen, in the form of air or moisture.

Other possibilities for exposure to oxygen are upon removal of the membrane from fluorination reactor and also prior to fluorination when air and moisture may be trapped in the polymer. These sources may all contribute in some way to the observed incorporation of oxygen groups during fluorination.

The most significant change on the surface following exposure to PFO plasma for 10 s is the appearance of a significant amount of fluorine; the XPS survey scan detects 52.3% fluorine, 46.5% carbon, and 1.2% oxygen (Table I). The nature of the 52.3% fluorine on the surface, following a 10-s PFO plasma exposure was characterized through the C_{1S} spectra (Fig. 3).

The changes in atomic composition correspond to the formation of pp-PFO film on the PEI substrate. The C content decreases from 83% for untreated PEI to ~45% after plasma treatment. The composition of the deposited layer pp-PFO is close to the composition of PFO ($C_8H_3F_{13}$), i.e., 38% carbon. The composition difference is partly due to the carbon contamination of the surface. The variation of pp-PFO molecular structure with exposure time can be described through the variation in the fluorine to carbon ratio (F/C).

The F/C ratios in Table I are calculated from the high resolution XPS spectra, and were estimated by using the conventional method[21] of the peaks area. The fluorine concentration (the F/C ratio) of the pp-PFO-PEI surface increases rapidly in the first few seconds of PFO plasma exposure, reaching 1.30. We notice that the F/C ratio in the deposited layer is weaker than the F/C ratio of about 1.6 in the monomer. In these conditions, the pp-PFO composition is ~56% F and 43% C.

The concentrations of CF_3, CF_2, *CF—CF_n, CF, and *C—CF in Table II are based on the relative peak area (where percentage is the concentration of atom group). pp -PFO for 480 s has a relatively high concentration in CF_2: 30.4%, about 12.5% in CF_3, and about 27.7% in ΣCF. The total CF, ΣCF, is the sum of the CF and *CF[sbonds]CF_n in Table II.

From the Table II results, we can consider that the PP mechanism is weakly related to the treatment time, leading to a pp-PFO deposited layer with practically the same chemical nature, however, with an increasing thickness. The thickness of the deposited layers has been estimated from SEM micrographs of the cross section of the samples treated for various times. So, the average of the percentage values (Table II) gives the typical atomic group composition of the pp-PFO layer.

The validity of these results was confirmed by results in Table III , in which the F and C contents derived from the curve fits in Table II are compared with those from the atomic composition analysis in

TABLE III
Comparison of F and C Contents from Tables I and II

Exposure time (s)	Chemical composition (%)			
	From XPS survey spectra[a]		From CIs deconvolution and eq. (1)	
	C	F	C	F
10	47.0	53.0	44.5	55.5
30	48.1	51.9	43.5	56.5
60	44.6	55.4	46.9	53.1
120	44.6	55.4	44.1	55.9
240	43.75	56.25	43.6	56.4
480	43.5	56.5	44.3	55.7

[a] Normalized to F+C=100%.

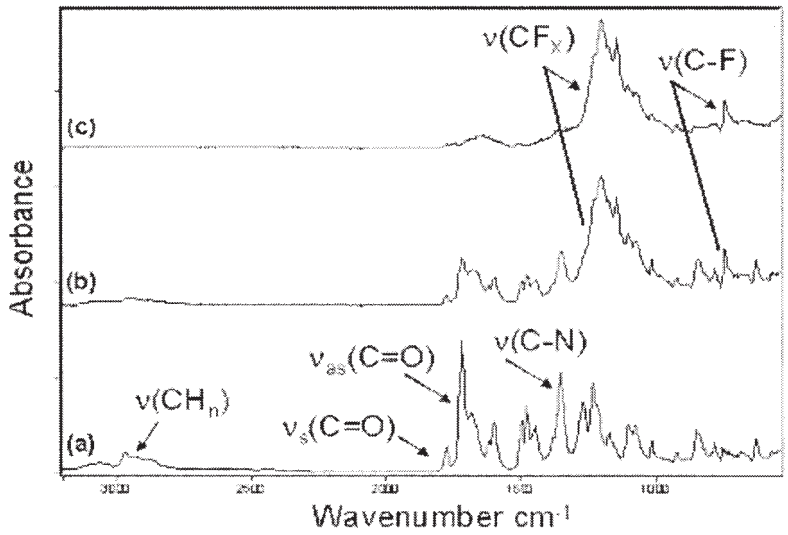

Figure 4 FTIR spectra of PEI (a) pp-PFO-PEI (b), pp-PFO (50 W, 10 s, 40 Pa) (c).

Table I. The F content was calculated from the results in Table II using the eq. (1),[13] which is only applicable when all the atoms are included within the C1S curve fit.

$$\%F = \frac{3\%(CF_3)+2\%(CF_2)+\%(CF)+\%(*CF-CF_n)}{3\%(CF_3)+2\%(CF_2)+\%(CF)+\%(*CF-CF_n)+\ 100} \times 100 \quad (1)$$

An alternative equation, which uses the experimental atomic concentration, was used when the above assumption was not valid. The eq. (1) is based solely on theory and is therefore a more sensitive test of its validity.

Table III presents the results from Table I normalized to F + C = 100% (the curve fit did not take the negligible amount of oxygen into account). Table III shows that there is an average variation in elemental concentrations between the results from Tables I and II, well within the experimental error.

FTIR-ATR

The presence of fluoro-polymer on the surface of treated PEI has also been identified by FTIR-ATR spectroscopy, as shown in Figure 4. For simplicity, the high wavenumber region of the IR spectra without absorption bands has been suppressed.

Infrared spectra are useful for qualitative characterization of plasma polymers. The comparison of the FTIR-ATR spectra of PEI [Fig. 4(a)] and pp-PFO-PEI [Fig. 4(b)] indicates that the enhanced absorption at 1000–1400 cm^{-1} observed in [Fig. 4(b)] is due to overlapping absorption of C—F of the [sond]CF$_x$ (x = 1–3) species' stretching modes.[22–24] The presence of CF$_x$ species in the plasma-polymerized PFO is consistent with the XPS result in Figure 3. The absorption band at 750 cm^{-1} could be related to the presence of "graphitic islands", as observed in amorphous carbon films.[25] However, given its narrow width, such a feature is more likely to be due to a mode of the fluorinated groups. These bands are missing in the IR spectra of untreated PEI [Fig. 4(a)]; however, characteristic absorption bands of PEI at 1721 and 1780 cm^{-1}, attributable to the in-phase and out-of-phase stretching vibrations of the carbonyl groups of the imide on five-membered ring,[26] and the band of C—N at 1367 cm^{-1}[27] are still visible in Figure 4(b), whereas the fluorinated deposit pp-PFO [Fig. 4(c)] shows only characteristic bands of the fluorinated species. A band centered at 3000 cm^{-1}, due to —CH$_n$ group stretching modes,[22–28] also becomes less evident when the fluorine content in the film increases.

In the ATR technique, the sample is placed in optical contact with an IRE. On total internal reflection, the field strength decays exponentially (the evanescent wave) from the interface into the sample. A nominal depth of penetration (d_p) is defined as the depth at which the field strength decreases to 1/e and is a function of the RI of the sample and the IRE, the angle of incidence, and the wavelength. Assuming an RI of 1.5, the d_p of a typical polymer in contact with a Si ATR crystal with 45° incidence is 0.85 μm at 1000 cm^{-1}. However, a significant portion of the evanescent wave penetrates perhaps 2–3 times deeper than does the nominal d_p. Taking this into consideration, it is reasonable to estimate that in pp-PFO-PEI [Fig. 4(b)] the graft thickness is somewhat less than, say, 2 μm, whereas in pp-PFO [Fig. 4(c)] the graft is around 2 μm or greater.

TABLE IV
Degree of Graft as Determined by FTIR

Exposure time (s)	Graft (mole ratio)
10	0.27
30	0.54
60	0.40
120	0.85
240	0.82
480	0.95

With care, semiquantitative analysis of the degree of fluorination is also possible from the Fourier transform infrared (FTIR) results using the assumption that the measured spectrum is a linear combination of the graft and substrate spectrum. The wavelength dependence of the penetration depth complicated matters, but the consequences were minimized by restricting the spectral region used in the analysis. Two spectra were used for calibration purposes: a spectrum of the ungrafted substrate for the zero mole fraction point and a spectrum of the most highly grafted sample for the 0.95 mole ratio point. The 0.95 mol ratio figure was estimated from the degree of carbonyl intensity persisting in the most highly grafted sample spectrum. The relative contribution of the substrate and graft spectrum to an average spectrum for each sample was calculated using the CLS function of the TQAnalyst program. The results are presented in Table IV.

Although the trend of increased fluorine content with increased exposure time is in general agreement with the XPS results, there are significant differences in the detail that probably arise from the different scope of the two techniques. XPS measures purely surface coverage, whereas in ATR the depth of penetration plays an important role in addition to the surface coverage, as discussed earlier. XPS results show that the 60- and 120-s exposure samples have similar high F/C ratios, suggesting high surface coverage in both samples. On the other hand, the FTIR results indicate that there is twice as much fluoro-polymer present after 120-s exposure than after 60-s exposure. A rationale for these two apparently contradictory results is that the fluoro/substrate ratio is the same for each graft, but the graft is twice as thick after 120-s exposure than after 60 s. This case illustrates the importance of performing both ATR and XPS measurements to gain a volumetric perspective of the nature of the graft.

The homogeneity of the grafts was measured by spectral mapping of a 500 × 500-μm^2 region on each sample. Gray scale maps of the degree of fluorination for the region were constructed by submitting the spectrum at each pixel to CLS analysis as outlined earlier. The highly exposed samples were very even. The 10-s exposure graft (see Fig. 5) was the least homogeneous and showed a gradient from 0.16 to 0.47 across the region as well as a single point where the graft is much higher than average. In light of the variation across the sample being quite large, single point measurements on these kinds of surfaces should be used with care.

Surface energy analysis

To complement the XPS and FTIR-ATR analyses and to provide additional data from the surface of the fluorinated layer, contact angles and surface energies were determined for membranes treated under the same fluorination conditions as earlier.

The surface energy (γ_S) and its polar and dispersive components, (γ_S^p) and (γ_S^d), were calculated from the contact angles for water and methylene iodide as described earlier. The measured value of γ_S for unfluorinated PEI is 46 mJ m^{-2}.

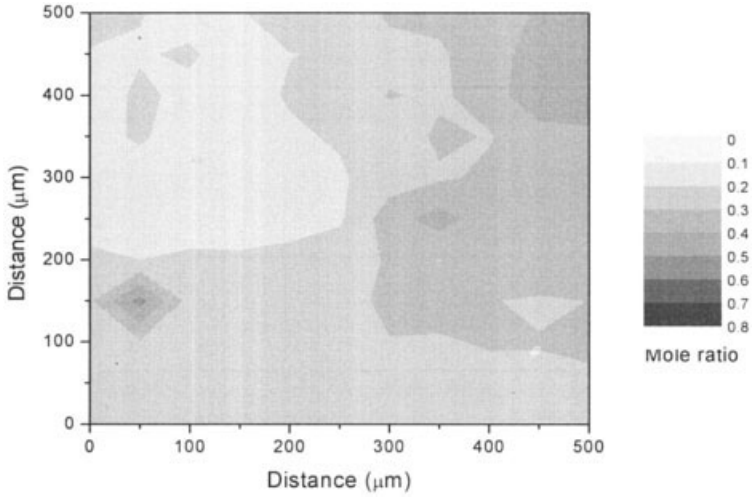

Figure 5 Gray scale map of a 500 × 500-μm region of the 10-s exposed film.

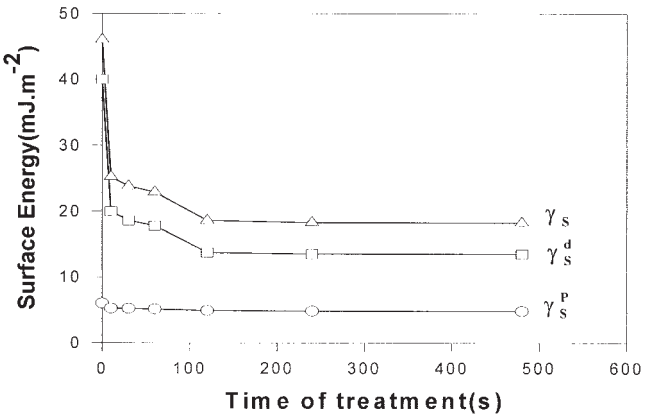

Figure 6 Evolution of surface energy and its dispersive and polar component of pp-PFO-PEI as function of the time of the treatment (50 W, 40 Pa).

Figure 6 shows the surface energy and its polar and dispersive components in response to fluorination treatment. Fluorination for various times gradually reduces the surface energy from 46 to 18.3 mJ m^{-2}, but the fluorination treatment longer than 120 s produces no further significant variation. Since the PFO layer was deposited on the surface, its chemical composition and texture approached a final state characterized by the lowest surface energy. It seems that the last value of γ_S could be related with the surface tension of the PFO monomer included in the range of 16–21 mJ m^{-2}.[29] The dispersive surface energy component γ_S^d strongly decreases with increase in fluorination time and the polar component γ_S^p is weaker, and its reduction for various times is 1.2 mJ m^{-2}.

Contact angle measurements with the storage time from day 1 to day 40 (atmospheric air, ambient temperature) led to very fixed values of the surface energy. So, the fluorinated-plasma treatment of PEI can be described as a permanent modification.

Finally, the reduction in surface energy of pp-PFO-PEI according to the processing time is due essentially to the formation of a fluorinated deposit on the surface, which increases its hydrophobicity. This drop of energy is related to the decrease in the dispersive component of the surface energy.

SEM

The surface topography is of great importance to the surface wettability of the polymer films.[30]

Figure 7(a,b) show the surface of the untreated sample PEI and PFO plasma treated sample pp-PFO-PEI (50 W, 10 s), respectively. It can be seen that there is a significant difference in surface topography between the untreated and treated sample. The untreated one has a rougher surface topography than does the plasma treated substrate; a smooth and dense surface was more apparent after plasma treatment. The smooth pp-PFO surface suggests that polymerization occurs predominantly on the substrate surface.[13] The polymer film grows through reaction with the monomer fragments that reach the surface.

Since the surface energy is also affected by the surface texture, it is very probable that this smooth surface also contributes to the low surface energies measured.

Figure 8(a–d) shows the SEM micrographs taken at the cross sections of samples untreated [Fig. 8(a)] and treated for 10 s [Fig. 8(b,c)] and for 480 s [Fig. 8(d,e)] under the RF power of 50 W at a magnification of 2000× [Fig. 8(b,d)] and 20,000× [Fig. 8(a,c,e)].

The SEM cross-sectional micrographs of the samples revealed continuous films with indication of modifications of appreciable thickness produced by the plasma [Fig. 8(b)] compared with the untreated sample [Fig. 8(a)].

Figure 8(d,e) clearly show the smooth and homogeneous coating on the surface of PEI. This cross-sectional thickness has increased in size compared with

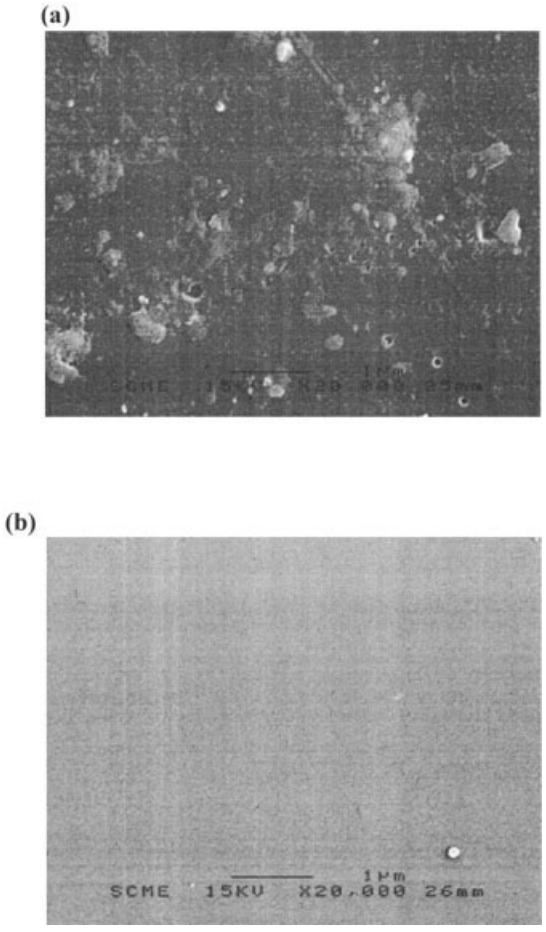

Figure 7 Scanning electron micrographs (magnification, 20 000×) of the surface of the untreated PEI film (a) and of the pp-PFO-PEI film (10 s, 50 W) (b).

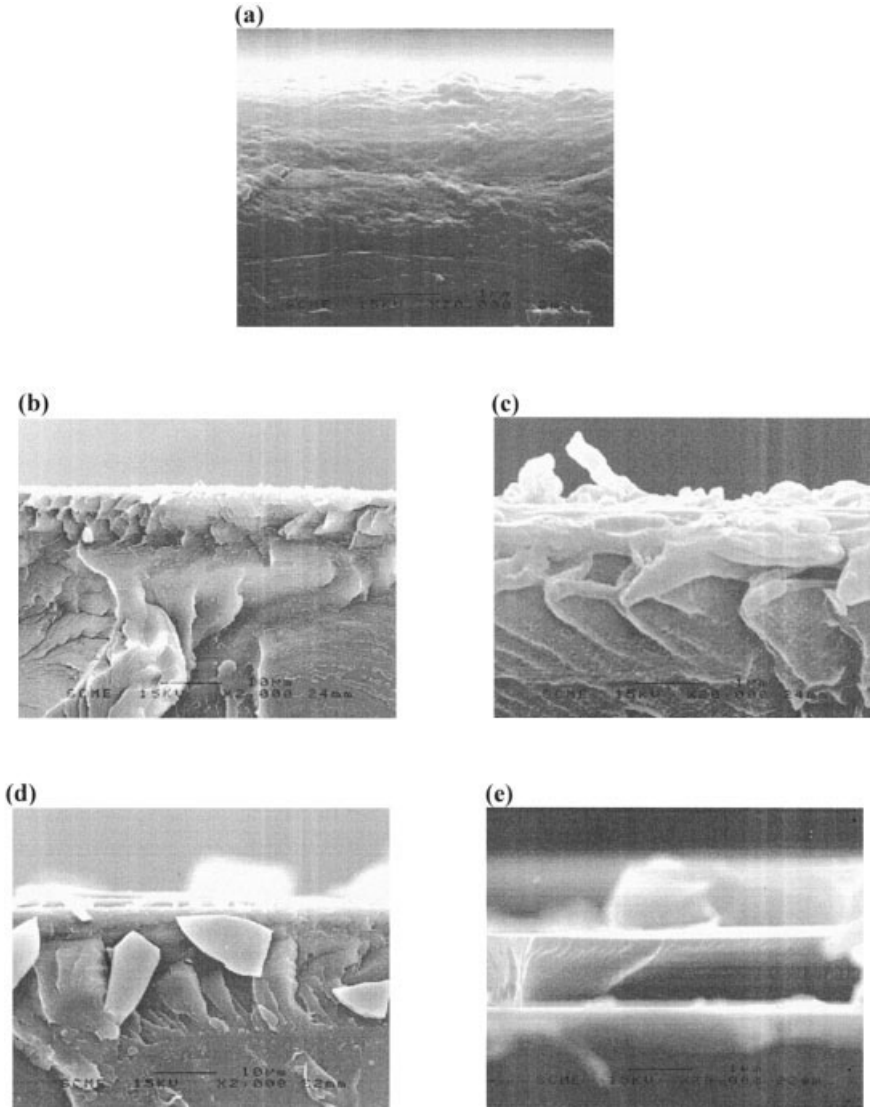

Figure 8 SEM micrographs of cut cross section of PEI film (a), and cut cross section of pp-PFO-PEI films for 10 s (b and c) and for 480 s (d and e).

that of the sample treated for 10 s [Fig. 8(b,c)], because when the plasma exposure time is 10 s, it is difficult to highlight the coating. On the other hand, for 480 s it can be seen that the fluorinated deposit is very thick and the surface becomes rigid and breakable. This coating has a thickness of about 1.2 μm [Fig. 8(e)].

CONCLUSIONS

The objective of this work was the surface treatment of Ultem 1000 films by fluorination plasma to increase their hydrophobicity and thus develop their application for the separation of the organic mixtures and the extraction of volatile micropollutants of water by pervaporation. Therefore, we used the PP of PFO to deposit a highly fluorinated and hydrophobic film on to Ultem 1000.

The effect of the plasma exposure time on surface composition and topography of the deposited PFO polymer films were studied by XPS, FTIR, surface energy analysis, and SEM. It was shown that increasing the fluorination times from 10 to 480 s resulted in an increased F/C ratio and a decrease in the surface energy γ_s from 46 to18.3 mJ m^{-2}.

References

1. Yasuda, H. Plasma Polymerization; Academic Press: New York, 1985.
2. Morosoff, N. In Plasma Deposition, Treatment, and Etching of Polymers; d'Agostino, R., Ed.; Academic Press: New York, 1990; p 1.
3. Han, L. C. M.; Timmons, R. B.; Lee, W. W. J Vac Sci Technol B 2000, 18, 799.

4. Chen, W.; Fadeev, A. Y.; Hseih, M. C.; Oner, D.; Youngblood, J.; McCathy, T. J. Langmuir 1999, 15, 3395.
5. Han, L. C. M.; Timmons, R. B.; Lee, W. W.; Chen, Y. Y.; Hu, Z. B. J Appl Phys 1998, 84, 439.
6. Coulson, S. R.; Woodward, I. S.; Badyal, J. P. S.; Brewer, S. A.; Willis, C. Langmuir 2000, 16, 6287.
7. Coulson, S. R.; Woodward, I. S.; Badyal, J. P. S.; Brewer, S. A.; Willis, C. Chem Mater 2000, 12, 2031.
8. Chen, W.; Fadeev, A. Y.; Hsieh, M. C.; Oner, D.; Youngblood, J.; McCarthy, T. J. Langmuir 1999, 15, 3395.
9. Schue, F.; Clarotti, G.; Sledz, J.; Mas, A.; Geckeler, K. E.; Gopel, W.; Orsetti, O. Makromol Chem Macromol Symp 1993, 73, 217.
10. Owens, D. K.; Wendt, R. C. J Appl Polym Sci 1969, 13, 1741.
11. Mohr, J. M.; Paul, D. R.; Pinnau, I.; Koros, W. J. J Membr Sci 1991, 56, 77.
12. Briggs, D. Handbook of X-Ray and Ultraviolet Photoelectron Spectroscopy; Heyden: London, 1978.
13. Sandrin, L.; Silverstein, M. S.; Sacher, E. Polymer 2001, 42, 3761.
14. Chen, R.; Silverstein, M. S. J Polym Sci Part A: Polym Chem 1996, 34, 207.
15. D'Agostino, R. In Plasma Deposition, Treatment and Etching of Polymers; D'Agostino, R., Ed.; Academic Press: New York, 1990; p 95.
16. Beamson, G.; Briggs, D. High Resolution XPS of Organic Polymers; Wiley: New York, 1992.
17. Ryan, M. E.; Fonseca, J. L. C.; Trasker, S.; Badyal, J. P. S. J Phys Chem 1995, 99, 7060.
18. Silverstein, M. S.; Sandrin, L.; Sacher, E. Polymer 2001, 42, 4299.
19. Le Roux, J. D.; Paul, D. R.; Arendt, M.; Yuan, Y.; Cabasso, I. J Membr Sci 1994, 94, 143.
20. Mohr, J. M.; Paul, D. R.; Taru, Y.; Mlsna, T.; Lagow, R. J. J Membr Sci 1991, 55, 149.
21. D'Agostino, R.; Lamendola, R.; Favia, P.; Giquel, A. J Vac Sci Technol A 1994, 12, 308.
22. Jacobsohn, L. G.; Franceschini, D. F.; Maria Da Costa, M.; Freire, F. L., Jr. J Vac Sci Technol A 2000, 18, 2230.
23. Lindon, J. C.; Tranter, G. E.; Holmes, J. L. Encyclopedia of Spectroscopy and Spectrometry; Academic Press: New York, 2000; Vol. 1.
24. Hacforth, H. L. Infrared Radiation; McGraw-Hill: New York, 1960; p 115.
25. Ogwu, A. A.; Lamberton, R. W.; Morley, S.; Maguire, P.; McLaughlin, J. Physica B 1999, 269, 335.
26. Socrates, G. Infrared Characteristic Group Frequencies; Wiley: Chichester, 1980.
27. Lee, K. W.; Kowalczyk, S. P.; Shaw, J. M. Macromolecules 1990, 23, 2097.
28. Dischler, B.; Bubenzer, A.; Koidl, P. Solid State Commun 1983, 48, 105.
29. Simons, J. H. U.S. Pat. 2,522,968 19,500,919 (1950).
30. Wenzel, R. N. Ind Eng Chem 1936, 28, 988.